RESEARCH ARTICLE | NOVEMBER 13 2023

Experimental evidence of hole injection through V-defects in long wavelength GaN-based LEDs

Saulius Marcinkevičius ; Jacob Ewing ; Rinat Yapparov ; Feng Wu; Shuji Nakamura ; James S. Speck

Appl. Phys. Lett. 123, 201102 (2023)
https://doi.org/10.1063/5.0179513
CHORUS

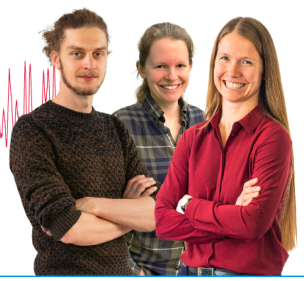

Applied Physics Letters ARTICLE pubs.aip.org/aip/apl

Experimental evidence of hole injection through V-defects in long wavelength GaN-based LEDs

Cite as: Appl. Phys. Lett. **123**, 201102 (2023); doi: 10.1063/5.0179513
Submitted: 3 October 2023 · Accepted: 2 November 2023 ·
Published Online: 13 November 2023

Saulius Marcinkevičius,[1,a)] Jacob Ewing,[2] Rinat Yapparov,[1] Feng Wu,[2] Shuji Nakamura,[2] and James S. Speck[2]

AFFILIATIONS

[1]Department of Applied Physics, KTH Royal Institute of Technology, AlbaNova University Center, 10691 Stockholm, Sweden
[2]Materials Department, University of California, Santa Barbara, California 93106, USA

[a)]Author to whom correspondence should be addressed: sm@kth.se

ABSTRACT

Hole injection through V-defect sidewalls into all quantum wells (QWs) of long wavelength GaN light emitting diodes had previously been proposed as means to increase efficiency of these devices. In this work, we directly tested the viability of this injection mechanism by electroluminescence and time-resolved photoluminescence measurements on a device in which QW furthest away from the *p*-side of the structure was deeper, thus serving as an optical detector for presence of injected electron–hole pairs. Emission from the detector well confirmed that, indeed, the holes were injected into this QW, which could only take place through the $\{10\bar{1}1\}$ V-defect sidewalls. Unlike direct interwell transport by thermionic emission, this transport mechanism allows populating all QWs of a multiple QW structure despite the high potential barriers in the long wavelength InGaN/GaN QWs.

Solid-state lighting based on red, green, and blue (RGB) GaN-based light emitting diodes (LEDs) has advantages in energy efficiency and flexibility in color tuning over the currently used blue LED and phosphor approach. Similarly for display applications, RGB micro-LEDs are potentially advantageous over liquid crystal or organic LEDs because of the much higher luminance, efficiency, and durability.[1] However, to realize these advantages, efficient red, green, and blue LEDs are needed. In blue LEDs, the peak electrical to optical power conversion efficiency (or wall plug efficiency, WPE) has reached ∼90%.[2] For green and especially red GaN LEDs, the WPE is much lower. The peak efficiency is typically reached at low current densities, a few A/cm^2, at which it is limited by the nonradiative Shockley–Read–Hall recombination in quantum wells (QWs) of the active region.[2] At large drive current densities required for high power applications, the nonradiative Auger recombination causing the efficiency droop sets in. This effect is more severe for a nonuniform interwell carrier distribution because of the fast Auger recombination in the highly populated wells. Due to the small effective mass, electron transport across the QWs is fast.[3] The nonuniform carrier distribution between the wells occurs due to the inefficient interwell hole transport.[3–5] The hole transport proceeds via thermionic emission, and already for relatively shallow $In_{0.12}Ga_{0.88}N$/GaN QWs emitting in the violet spectral region the hole transport across the QWs is slow.[6] For blue and especially much deeper green- and red-emitting InGaN/GaN QWs, the effect of the poor interwell transport on the interwell carrier distribution and high power LED operation should be even more severe.[3]

However, a few recent papers have reported long wavelength GaN LEDs with exceptionally high peak WPE, ∼30% for devices emitting in the yellow spectral region.[7,8] It has been proposed that such high efficiency might be related to the carrier injection into all QWs of the active region (eight or nine in Refs. 7 and 8) via V-defects.[9] Such defects form in polar GaN at threading dislocations and/or In-rich clusters and have shapes of inverted hexagonal pyramids.[10] In QW structures, polar QWs in the bulk of the structure transform into semipolar wells on the $\{10\bar{1}1\}$ facets of the V-defects. The thickness and indium content in the semipolar QWs are much smaller than in the polar ones;[11] hence, their band potentials are higher. Such band alignment should allow hole injection from the *p*-side of the structure into the polar QWs through the semipolar sidewall QWs.[9,12,13] However, since the results of Refs. 7 and 8 have been obtained on LEDs with identical QWs, there is no direct experimental evidence that LED emission originates from all and not just a few QWs located closest to the *p*-side of the structure. In this Letter, we present a direct experimental proof that the hole injection via V-defects indeed takes place.

To test whether electrically injected holes populate all QWs, an LED with non-identical QWs in the active region was grown. The QW closest to the *n*-side of the structure had a larger In content and width, which shifted its emission spectrum to the red and allowed distinguishing this deeper QW (or a detector QW, DQW) from the other wells spectrally [Fig. 1(a)]. Being on the *n*-side, the DQW was populated by electrons; hence, its emission would be a proof that holes also populate this QW. The hole transport path from the *p*-side could be evaluated by time-resolved photoluminescence (PL) using the optical marker technique, which allows tracking dynamics of the interwell carrier transport toward the DQW.[6,14–16]

The structure of the studied LED is shown in Fig. 1(b). Starting from the substrate, the device contains a 2 μm thick unintentionally *n*-doped (UID) GaN layer that buries impurities and defects from the substrate interface, and Si-doped GaN contact layers. The subsequent 20 period GaN/$In_{0.05}Ga_{0.95}N$ superlattice serves to nucleate large V-defects[17,18] and capture point defects before the growth of the active region.[19] The active region contains three $In_xGa_{1-x}N$ QWs [Fig. 1(a)],

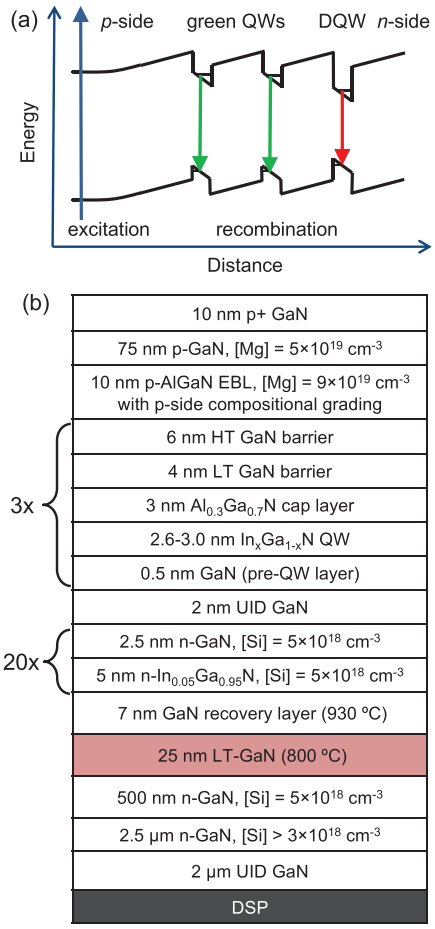

FIG. 1. Schematics of the LED active region. The blue arrow indicates optical excitation, green and red arrows—recombination in the green and detector QWs, respectively (a). LED structure (b). Abbreviations: DSP—double side polished (sapphire), UID—unintentionally (*n*-) doped, HT—high temperature, LT—low temperature, and EBL—electron blocking layer.

two of which with $x = 0.20$ are 2.6 nm thick and emit in the green, and one, the DQW, ($x = 0.22$, thickness 3.0 nm)—in the red. The QWs are separated by 10.5 nm thick GaN barriers and 3 nm $Al_{0.30}Ga_{0.70}N$ interlayers. The purpose of the interlayers is to suppress In desorption from QWs that are grown at a lower temperature than barriers.[20] The top part of the structure includes a 10 nm *p*-AlGaN electron blocking layer and 85 nm thick *p* and p^+ GaN contact layers. The structure was grown on a double side polished sapphire substrate. The choice of the substrate, even though not optimal for the far-field measurements because of the Fabry–Pérot oscillations modulating the optical spectra, was made for the sake of future near-field spectroscopy measurements. Structure parameters were determined by cross-sectional high angle annular dark field scanning transmission electron microscopy (HAADF-STEM) and energy-dispersive x-ray spectroscopy (EDS). Electroluminescence (EL) of the LED was studied on wafer using needle contact probes.

To verify the hole transport across the green QWs to the DQW, two types of experiments were performed. One was measurement of EL spectra, and the other measurement of time resolved PL at the DQW peak energy. In both experiments, spectra were recorded with a 0.5 m spectrometer with a liquid N_2 cooled CCD detector. For the time-resolved PL, carriers were excited by 200 fs pulses at a 260 nm central wavelength generated by a self-mode-locking Ti:sapphire laser and third harmonic generator. Because of the long PL decay times, the original laser pulse repetition rate of 80 MHz was reduced to 4 MHz with an acousto-optic pulse picker. PL dynamics was measured by a time-correlated single photon counter (temporal response 50 ps) after selecting emission from particular QWs (green or red) by bandpass filters. Most of the carriers were excited in the *p*-side layers since for the 260 nm excitation the absorption length is ~50 nm. The pulse energy density was 15 $\mu J/cm^{-2}$, which corresponds to the photoexcited carrier density in the GaN layers just after a pulse of about $2 \times 10^{18}\,cm^{-3}$. Lateral atom force microscopy (AFM) scans were performed in the Quantitative Imaging mode using JPK NanoWizard 3. Cross-sectional HAADF-STEM images and EDS chemical element maps were obtained with a Talos G2 200× TEM/STEM system equipped with ChemiSTEM EDS, operated at 200 kV.

Figure 2(a) displays an AFM map of our sample. One can notice large and small V-defects. The large ones form in the LT-GaN layer or superlattice and are believed to serve as hole injectors; the small ones originate in the active region and have an enhanced rate of the nonradiative recombination.[11,17,18] The density and diameter of the V-defects can, to some extent, be controlled by the growth conditions and structure parameters.[10,21] Generally, higher growth rates and kinetically limited growth conditions favor the formation of the V-defects. In more detail, structure of the V-defects in similar LEDs is described in Ref. 17.

Figure 2(b) shows a cross-sectional HAADF-STEM image of the structure in the vicinity of a V-defect. The three active region QWs and semipolar QWs on the V-defect sidewall can be seen on the left-hand side of the image. The right top corner depicts the contact metal filling of the V-defect. Hole transport paths from *p*-GaN to the DQW are schematically shown by arrows: directly across the green QWs (1) and via the semipolar QWs at the V-defect facet (2).

Room temperature EL spectra at different bias values are displayed in Fig. 3. The spectra contain peaks from both the green (at ~515 nm at higher biases) and red (650 nm) QWs. In similar LED

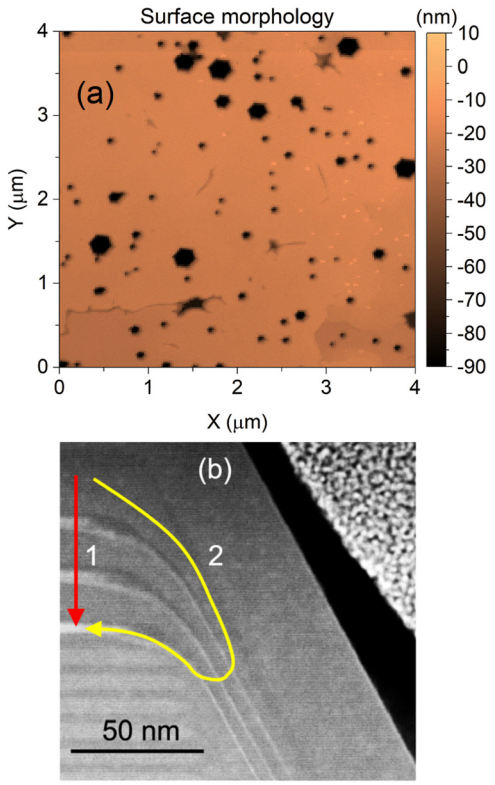

FIG. 2. AFM image of the LED structure displaying small and large hexagonal V-defects (a). Cross-sectional HAADF-STEM image of the structure in the vicinity of a large V-defect with schematically illustrated paths of the hole transport toward the DQW directly across the green QWs (1) and via semipolar QWs at the V-defect facets (2) (b).

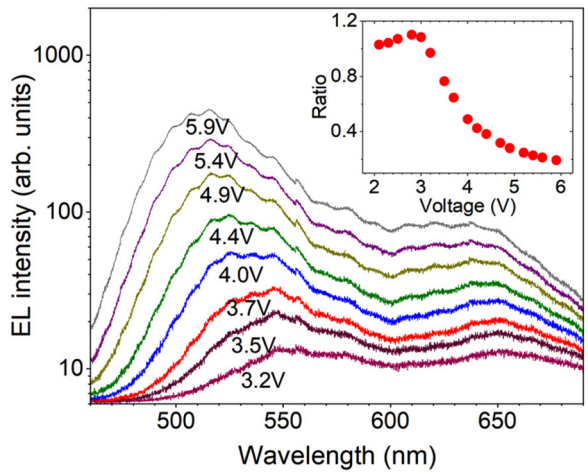

FIG. 3. EL spectra at different bias voltages. The inset shows the spectrally integrated EL intensity ratio for the green and detector QW peaks as a function of the applied bias.

structures with all identical QWs in the active region, the red EL peak has not been observed. The sheer presence of the red EL peak confirms that holes do reach the DQW from the *p*-side. Below we will discuss the mechanism of the hole transport to the DQW.

The hole transport can either take place directly across the green QWs [path 1, Fig. 2(b)] or via the V-defect semipolar QWs, bypassing the green QWs [path 2, Fig. 2(b)]. The direct hole transport would take place via subsequent capture to and thermionic emission out of the green QWs until the DQW is reached.[6,22,23] Other transport mechanisms, such as ballistic hole transport over the QWs and tunneling though the barriers can be ruled out. The ballistic transport—because the hole mean free path at room temperature is much shorter than the barrier width,[24] and tunneling—because the 13 nm barriers are too thick.[6] The thermionic hole transport time, which is already long for relatively shallow $In_{0.12}Ga_{0.88}N$/GaN QWs (1–10 ns),[6] depends exponentially on the barrier height; thus, for the deep $In_{0.20}Ga_{0.80}N$/GaN QWs of our device the thermionic transport is unlikely. Nevertheless, to have a clear experimental proof, we have tested this possibility by measuring the PL dynamics.

First, let us examine time-integrated PL and EL spectra measured at 3.5 V bias, at which the device is close to flat-band conditions but not yet emitting strong EL (Fig. 4). In the spectrum, the green QW PL intensity is considerably larger than that of the DQW. This is different from the EL spectrum in which intensities of the green QW and DQW peaks are similar. This difference is related to the different hole transport mechanisms as will be discussed below. A weak PL peak at ~440 nm (not shown in Fig. 4) due to recombination in the sidewall semipolar QWs[25] has also been observed.

QW PL transients consist of a sharp rise and gradual decay with decay times of 3.2 and 6.5–7.0 ns for the green and detector QWs, respectively. The transients for the DQW are shown in Fig. 5. In the method of optical marker, information about the carrier transport is obtained from the dynamics of the DQW PL rise. Here, two contributions should be distinguished—a fast and slow one. The fast rise component reflects the direct carrier excitation in the DQW and adjacent barriers. Since the excitation intensity in a material decreases with distance exponentially, some of the direct photoexcitation is unavoidable, even for thick cap layers. The fast rise time is determined by the carrier

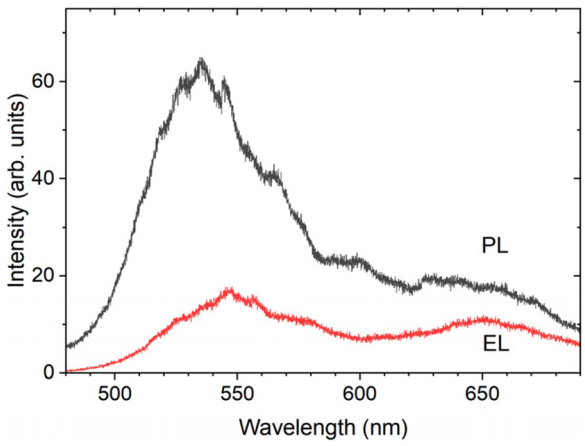

FIG. 4. EL (red curve) and PL (black curve) spectra measured at 3.5 V forward bias.

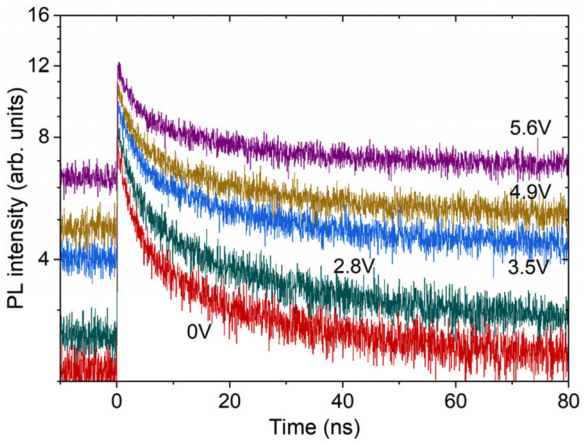

FIG. 5. Detector QW PL transients at different bias values.

relaxation in the DQW and capture from the barriers. These processes take $\lesssim 1$ ps,[26] well below our temporal resolution, and in Fig. 5 is perceived as instantaneous. The slow rise component, if present, is caused by the radiative recombination of carriers arriving to the DQW after excitation outside the DQW, typically in the cap layer. The slow rise time reflects the time of the carrier transport to the DQW. For shallow GaAs- or InP-based QWs, the slow rise time is of the order of tens to hundreds of ps;[14,16] for much deeper nitride QWs—it is several to tens of ns.[3]

As can be judged from Fig. 5, the DQW PL transient contains only the fast rise component. The absence of the slow rise component confirms that the vertical thermionic interwell transport [path 1 in Fig. 2(b)] does not take place. On the other hand, the presence of the DQW EL and PL peaks (Figs. 3 and 4) is the evidence that holes do arrive from the *p*-side of the structure to the DQW. Since holes cannot reach the DQW via the thermionic interwell transport, the only viable transport mechanism is via the semipolar sidewall QWs [or path 2 of Fig. 2(b)].

Comparison of the green QW and DQW peaks of the EL and PL spectra (Fig. 4) indicates that hole transfer into the DQW is more efficient in the case of the electrical carrier injection. The difference between these injection mechanisms is the following: In the EL case, only holes should be transported from the *p*-side of the structure to the DQW. For PL, the transport mechanism is ambipolar diffusion since the photoexcited carrier density is higher than the density of holes induced by doping.[14] The less-efficient transfer of the photoexcited electron–hole pairs is probably related to the short electron lifetime in *p*-GaN. Our recent time-resolved PL measurements have shown that in *p*-GaN photoexcited electron–hole pairs recombine in 150 ps.[27] In addition, a considerable fraction of electrons is trapped to nitrogen vacancies within 20 ps. Using these trapping and recombination times and the ambipolar diffusion coefficient of 1.6 cm^2/s (Ref. 28), the corresponding distances of the lateral carrier diffusion would be 60 and 150 nm, respectively. Even considering the larger value of 150 nm as the distance from which carriers are captured to the large V-defects, the region from which carriers would be collected into the V-defects is small, about 10% of the total sample area. This explains the poor collection of photoexcited electron–hole pairs into the DQW. On the other hand, photoexcited carrier capture into the first green QW takes place after vertical transport of several tens of nm; thus, more carriers would by captured to the first green QW than to the semipolar V-defect QWs.

Returning to the dependence of the EL spectra on bias (Fig. 3), one can notice (i) a blue shift of the QW peaks (more pronounced for the green QWs than for DQW) and (ii) a nonlinear dependence of the green and detector QW EL intensity ratio (inset to Fig. 3). The shift can be assigned to the screening of the QW electric field and band filling of localized states,[29,30] which are more pronounced for the green QWs with a larger carrier concentration. The more rapid increase in the green QW EL intensity with bias probably occurs due to a faster direct hole transfer from the *p*-side to the first green QW at large forward bias thus limiting the number of holes available for transport to the DQW via the V-defects.

In conclusion, by performing EL and time-resolved PL measurements on long wavelength InGaN multiple QW LEDs with a detector QW, we have experimentally proved existence of the hole injection mechanism via semipolar QWs located on the facets of the V-defects. Unlike direct interwell transport by thermionic emission, this transport mechanism allows populating all QWs of a multiple QW structure in spite of the high potential barriers in the long wavelength InGaN/GaN quantum wells.

We would like to thank Prattakorn Metem for help with the AFM measurements. The research at KTH has been financially supported by the Swedish Energy Agency (Project No. P2022-00251). This work at UCSB was supported by the Solid State Lighting and Energy Electronics Center (SSLEEC), the Simons Foundation [Grant Nos. 601952 (J.S.S.), 601954 (C.W), and 1027114 (C.W.)], the National Science Foundation (NSF) RAISE program (Grant No. DMS-1839077), the U.S. Department of Energy under Award No. DE-EE0009691 (J.S.S. and C.W.), and the Sandia National Laboratories (Award No. 2150283).

AUTHOR DECLARATIONS

Conflict of Interest

The authors have no conflicts to disclose.

Author Contributions

Saulius Marcinkevicius: Conceptualization (lead); Data curation (equal); Formal analysis (equal); Funding acquisition (equal); Investigation (equal); Methodology (lead); Project administration (equal); Resources (equal); Supervision (equal); Visualization (equal); Writing – original draft (lead); Writing – review & editing (lead). **Jacob J. Ewing:** Data curation (equal); Investigation (equal); Methodology (equal); Writing – original draft (supporting). **Rinat Yapparov:** Data curation (equal); Formal analysis (equal); Investigation (equal); Methodology (equal); Visualization (supporting). **Feng Wu:** Data curation (equal); Formal analysis (equal); Investigation (equal); Methodology (equal); Visualization (supporting). **Shuji Nakamura:** Methodology (equal); Supervision (supporting). **James S. Speck:** Funding acquisition (equal); Project administration (equal); Resources (equal); Supervision (equal); Writing – original draft (supporting); Writing – review & editing (supporting).

DATA AVAILABILITY

The data that support the findings of this study are available from the corresponding author upon reasonable request.

REFERENCES

[1]J. Y. Lin and H. X. Jiang, Appl. Phys. Lett. **116**, 100502 (2020).
[2]C. Weisbuch, ECS J. Solid State Sci. Technol. **9**, 016022 (2020).
[3]D. S. Sizov, R. Bhat, A. Zakharian, K. Song, D. E. Allen, S. Coleman, and C. Zah, IEEE J. Sel. Top. Quantum Electron. **17**, 1390 (2011).
[4]A. David, M. J. Grundmann, J. F. Kaeding, N. F. Gardner, T. G. Mihopoulos, and M. R. Krames, Appl. Phys. Lett. **92**, 053502 (2008).
[5]W. G. Scheibenzuber and U. T. Schwarz, Appl. Phys. Express **5**, 042103 (2012).
[6]S. Marcinkevičius, R. Yapparov, L. Y. Kuritzky, Y.-R. Wu, S. Nakamura, S. P. DenBaars, and J. S. Speck, Appl. Phys. Lett. **114**, 151103 (2019).
[7]F. Jiang, J. Zhang, L. Xu, J. Ding, G. Wang, X. Wu, X. Wang, C. Mo, Z. Quan, X. Guo, C. Zheng, S. Pan, and J. Liu, Photonics Res. **7**, 144 (2019).
[8]S. Zhang, J. Zhang, J. Gao, X. Wang, C. Zheng, M. Zhang, X. Wu, L. Xu, J. Ding, Z. Quan, and F. Jiang, Photonics Res. **8**, 1671 (2020).
[9]Z. Quan, L. Wang, C. Zheng, J. Liu, and F. Jiang, J. Appl. Phys. **116**, 183107 (2014).
[10]X. H. Wu, C. R. Elsass, A. Abare, M. Mack, S. Keller, P. M. Petroff, S. P. DenBaars, J. S. Speck, and S. J. Rosner, Appl. Phys. Lett. **72**, 692 (1998).
[11]R. Yapparov, Y. C. Chow, C. Lynsky, F. Wu, S. Nakamura, J. S. Speck, and S. Marcinkevičius, J. Appl. Phys. **128**, 225703 (2020).
[12]C.-K. Li, C.-K. Wu, C.-C. Hsu, L.-S. Lu, H. Li, T.-C. Lu, and Y.-R. Wu, AIP Adv. **6**, 055208 (2016).
[13]C. H. Ho, J. S. Speck, C. Weisbuch, and Y.-R. Wu, Phys. Rev. Appl. **17**, 014033 (2022).
[14]B. Lambert, B. Deveaud, A. Chomette, A. Regreny, and B. Sermage, Semicond. Sci. Technol. **4**, 513 (1989).
[15]H. Hillmer, A. Forchel, T. Kuhn, G. Mahler, and H. P. Meier, Phys. Rev. B **43**, 13992 (1991).
[16]K. Fröjdh, S. Marcinkevičius, U. Olin, C. Silfvenius, B. Stålnacke, and G. Landgren, Appl. Phys. Lett. **69**, 3695 (1996).
[17]F. Wu, J. Ewing, C. Lynsky, M. Iza, S. Nakamura, S. P. DenBaars, and J. S. Speck, J. Appl. Phys. **133**, 035703 (2023).
[18]J. Ewing, C. Lynsky, J. Zhang, P. Shapturenka, M. Wong, J. Smith, M. Iza, J. S. Speck, and S. P. DenBaars, Crystals **12**, 1216 (2022).
[19]C. Haller, J.-F. Carlin, G. Jacopin, D. Martin, R. Butté, and N. Grandjean, Appl. Phys. Lett. **111**, 262101 (2017).
[20]J.-I. Hwang, R. Hashimoto, S. Saito, and S. Nunoue, Appl. Phys. Express **7**, 071003 (2014).
[21]I.-H. Kim, H.-S. Park, Y.-J. Park, and T. Kim, Appl. Phys. Lett. **73**, 1634 (1998).
[22]M. F. Schubert, J. Xu, Q. Dai, F. W. Mont, J. K. Kim, and E. F. Schubert, Appl. Phys. Lett. **94**, 081114 (2009).
[23]R. Yapparov, C. Lynsky, Y. C. Chow, S. Nakamura, J. S. Speck, and S. Marcinkevičius, Proc. SPIE **12001**, 1200104 (2022).
[24]S. Marcinkevičius, R. Yapparov, L. Y. Kuritzky, Y.-R. Wu, S. Nakamura, and J. S. Speck, Phys. Rev. B **101**, 075305 (2020).
[25]Y. C. Chow, T. Tak, F. Wu, J. Ewing, S. Nakamura, S. P. DenBaars, Y.-R. Wu, C. Weisbuch, and J. S. Speck, Appl. Phys. Lett. **123**, 091103 (2023).
[26]Ü. Özgür, M. J. Bergmann, H. C. Casey, Jr., H. O. Everitt, A. C. Abare, S. Keller, and S. P. DenBaars, Appl. Phys Lett **77**, 109 (2000).
[27]S. Marcinkevičius, Y. C. Chow, S. Nakamura, and J. S. Speck, J. Appl. Phys. **134**, 085703 (2023).
[28]P. Ščajev, K. Jarašiūnas, S. Okur, Ü. Özgür, and H. Morkoç, J. Appl. Phys. **111**, 023702 (2012).
[29]Y. Yang, X. A. Cao, and C. H. Yan, Proc. SPIE **7231**, 72310W (2009).
[30]D. F. Feezell, J. S. Speck, S. P. DenBaars, and S. Nakamura, J. Disp. Technol. **9**, 190 (2013).